Amplification of *PVT1* Contributes to the Pathophysiology of Ovarian and Breast Cancer

Yinghui Guan,[1] Wen-Lin Kuo,[1] Jackie L. Stilwell,[5] Hirokuni Takano,[6] Anna V. Lapuk,[1] Jane Fridlyand,[7] Jian-Hua Mao,[3] Mamie Yu,[4] Melinda A. Miller,[8] Jennifer L. Santos,[9] Steve E. Kalloger,[10] Joseph W. Carlson,[1] David G. Ginzinger,[3] Susan E. Celniker,[1] Gordon B. Mills,[11] David G. Huntsman,[10] and Joe W. Gray[1,5]

Abstract

Purpose: This study was designed to elucidate the role of amplification at 8q24 in the pathophysiology of ovarian and breast cancer because increased copy number at this locus is one of the most frequent genomic abnormalities in these cancers.

Experimental Design: To accomplish this, we assessed the association of amplification at 8q24 with outcome in ovarian cancers using fluorescence *in situ* hybridization to tissue microarrays and measured responses of ovarian and breast cancer cell lines to specific small interfering RNAs against the oncogene *MYC* and a putative noncoding RNA, *PVT1*, both of which map to 8q24.

Results: Amplification of 8q24 was associated with significantly reduced survival duration. In addition, small interfering RNA – mediated reduction in either *PVT1* or *MYC* expression inhibited proliferation in breast and ovarian cancer cell lines in which they were both amplified and overexpressed but not in lines in which they were not amplified/overexpressed. Inhibition of *PVT1* expression also induced a strong apoptotic response in cell lines in which it was overexpressed but not in lines in which it was not amplified/overexpressed. Inhibition of *MYC*, on the other hand, did not induce an apoptotic response in cell lines in which *MYC* was amplified and overexpressed.

Conclusions: These results suggest that *MYC* and *PVT1* contribute independently to ovarian and breast pathogenesis when overexpressed because of genomic abnormalities. They also suggest that *PVT1*-mediated inhibition of apoptosis may explain why amplification of 8q24 is associated with reduced survival duration in patients treated with agents that act through apoptotic mechanisms.

Authors' Affiliations: [1]Life Sciences Division, Lawrence Berkeley National Laboratory, Berkeley, California; [2]Department of Laboratory Medicine, [3]Cancer Research Institute, and [4]Department of Neurosurgery Research, University of California at San Francisco, San Francisco, California; [5]Trubion Pharmaceuticals, Seattle, Washington; [6]Department of Obstetrics and Gynecology, Jikei University School of Medicine, Tokyo, Japan; [7]Genentech, Inc., South San Francisco, California; and [8]Centre for Translational and Applied Genomics; [9]Cheryl Brown Ovarian Cancer Outcomes Unit of the British Columbia Cancer Agency; [10]Department of Pathology, University of British Columbia, Vancouver General Hospital and British Columbia Cancer Agency, Vancouver, British Columbia, Canada; and [11]Department of Molecular Therapeutics, M. D. Anderson Cancer Center, Houston, Texas

Received 12/5/06; revised 5/4/07; accepted 7/13/07.

Grant support: Office of Biological and Environmental Research, Office of Science, U.S. Department of Energy contract DE-AC03-76SF00098; NIH, National Cancer Institute grants CA58207, CA83639, and CA64602 and the Avon Foundation (JW. Gray).

The costs of publication of this article were defrayed in part by the payment of page charges. This article must therefore be hereby marked *advertisement* in accordance with 18 U.S.C. Section 1734 solely to indicate this fact.

Note: Supplementary data for this article are available at Clinical Cancer Research Online (http://clincancerres.aacrjournals.org/).

The content of this publication does not necessarily reflect the views or policies of the Department of Health and Human Services, nor does mention of trade names, commercial products, or organization imply endorsement by the U.S. Government.

Requests for reprints: Joe W. Gray, Life Sciences Division, Lawrence Berkeley National Laboratory, One Cyclotron Road, MS977/225A, Berkeley, CA 94720. Phone: 510-495-2438; Fax: 510-495-2535; E-mail: jwgray@lbl.gov.

doi:10.1158/1078-0432.CCR-06-2882

Amplification of a region on chromosome 8q24 is one of the most frequent events in carcinomas, including serous ovarian and breast cancers, and has been associated with reduced survival duration in some studies (1, 2). The well-established oncogene *MYC* maps to this locus and likely contributes to the pathophysiology of cancers in which it is amplified. However, the *PVT1* transcript also maps to this region and has been implicated in cancer pathophysiology as well (3). In mouse, for example, the *pvt-1* locus is a site of recurrent translocation in plasmacytomas (4, 5) and is a common site of tumorigenic retroviral insertion in lymphomas (6). In humans, the region homologous to *pvt-1* is a site of recurrent translocation between chromosomes 2 and 8 (7, 8) and its first exon is coamplified with *MYC* in colon carcinoma cell lines (9). *PVT1* has been suggested as a *MYC* activator (10); however, little evidence exists to support that role. Moreover, evidence is now emerging that *PVT1* may act as a noncoding RNA[12] that is strongly conserved between mouse and human.

We now present evidence that both *PVT1* and *MYC* contribute to ovarian and breast cancer pathophysiology when

[12] Huppi et al., personal communication.

overexpressed by amplification at 8q24. First, we show that amplification at this locus is associated with reduced survival duration in ovarian cancer. We also show that down-regulation of either *PVT1* or *MYC* expression using small interfering RNA (siRNA) technology inhibits proliferation in ovarian and breast cancer cell lines in which they are amplified and overexpressed but not in cell lines in which they are not overexpressed. In addition, we show that inhibition of *PVT1* but not *MYC* induces an amplification/overexpression-specific apoptotic response. Our analyses of *PVT1* transcripts are consistent with the interpretation that *PVT1* exerts its pathophysiologic influence as a noncoding RNA.[12]

Materials and Methods

Cancer cell lines. Ovarian cancer cell lines with and without amplification at 8q24 were selected from a collection of 30 cell lines that were either purchased from the American Type Culture Collection, European Collection of Cell Culture, German Resource Centre for Biological Material, and Interlab Cell Line Collection or generously provided by Drs. Gordon Mills and Robert Bast (M. D. Anderson Cancer Center, Houston, TX), Dr. Tom Hamilton (Fox Chase Cancer Center, Philadelphia, PA), Dr. Nelly Auersperg (University of British Columbia, Vancouver, British Columbia, Canada), and National Cancer Institute Drug Panel (listed in Supplementary Table S1). The known biological properties of the cell lines are summarized in Supplementary Table S1. Breast cancer cell lines with and without amplification at 8q24 were selected from a collection of 51 well-characterized lines described by Neve et al. (11).

Nucleic acid extraction. Genome DNA and total RNA were purified from cultured cells as described previously (11). Total RNA from a panel of normal human tissues was purchased from Clontech and used to measure relative expression levels of *PVT1*.

Genome copy number and expression analysis. Relative genome number was assessed in the 30 ovarian cell lines using array comparative genomic hybridization with three bacterial artificial chromosome (BAC) arrays as described previously (12, 13). These included (*a*) Hum2.0 arrays composed of 2,465 BACs selected at approximately megabase intervals along the genome (12, 14), (*b*) arrays composed of 1,860 BACs selected to include genes known to be involved in cancer pathogenesis (15), and (*c*) arrays carrying 400 BACs selected to tile across 13 Mbp at 3q26, 15 Mbp at 8q24, and 30 Mbp at 20q centered on regions of recurrent amplification associated with reduced survival duration in earlier studies (15). Global gene expression was assessed by hybridization to Affymetrix U133A arrays in the J. David Gladstone Institutes in the University of California at San Francisco as described.[13] Hybridized arrays were visualized with Affymetrix Microarray Suite 5.0. The image files of all the arrays were then analyzed together with the robust multiarray average algorithms (16). Genome copy number and expression analyses of the breast cancer cell lines used in this study are described by Neve et al. (11).

Real-time quantitative PCR analysis. Quantitative PCR (QPCR) was done essentially as described previously (17). Quantitative detection of specific nucleotide sequences was based on the fluorogenic 5′ nuclease assay and relative expression was calculated as described (17). Assays were purchased as Assays-on-Demand from Applied Biosystems. The catalogue numbers of these assays are listed in Supplementary Table S2. The sequences of PCR primers and Taqman probe specific for *PVT1* transcription unit were designed with ABI Primer Express 2.0 software based on the sequence of a published expressed sequence tag (EST) clone for human *PVT1* (National Center for Biotechnology Information accession no. M34428). The primer sequences for PVT1 were CATCCGGCGCTCAGCT (sense) and TCATGATGGCTGTATGTGCCA (antisense). The Taqman probe was 5′-FAM-CTGACCATACTCCCTG-GAGCCTTCTCC-BHQ1-3′. Primer and probe concentrations of 500 and 200 nmol/L were used, respectively. "No reverse transcriptase" analyses were done on all samples to confirm that genomic DNA was not present. For normalization, cDNA equivalent to the amount of RNA used in target gene measurements was measured for ribosomal 18S, glyceraldehyde-3-phosphate dehydrogenase, and cyclophilin A.

Transfection of siRNA. siRNAs against *PVT1* and *MYC* were either designed using the "BioTool" function available online[14] and purchased from Integrated DNA Technologies or ordered from Dharmacon Predesigned siGENOME Collection. Two siRNAs cognate to different parts of mRNA sequence of *PVT1* (siPVT1a and siPVT1b) and two siRNAs cognate to different parts of *MYC* (siMYCa and siMYCb) were used in this study. The target sequence of siPVT1a was 5′-CAGCCAT-CATGATGGTACT-3′ and that of siPVT1b was 5′-GGCACATTTCAGGA-TACTA-3′. The target sequence of siMYCa was 5′-GAGGCGAACACACA-ACGUC-3′. siMYCb was predesigned by Dharmacon (siGENOME ON-TARGET duplex 17, MYC) and its target sequence was 5′-GGAC-TATCCTGCTGCCAAG-3′. CY3-conjugated siRNA against *Aequorea* green fluorescent protein (siGFP) was designed and synthesized by Integrated DNA Technologies and used as a control for both transfection efficiency and nonsequence-specific siRNA effects. A predesigned control siRNA (siControl) from Dharmacon was also used as a second nonsequence-specific effect control.

Approximately 5×10^4 cells were plated to each well of a 24-well plate at least 24 h before transfection to achieve 50% to 70% confluency. siRNA transfection was done with LipofectAMINE 2000 (Invitrogen) following the manufacturer's instructions. Cells were harvested or fixed 8, 24, and/or 48 h after transfection for RNA, protein, cell cycle distribution, cell viability, and apoptosis analyses.

MYC Western blotting. Total protein sample (10 μg) was resolved in a precast NuPage 4% to 12% Bis-Tris Gel (Invitrogen), electrophoresed at 200 V for 45 min, and transferred to a piece of Immobilon transfer membrane at 250 mA for 50 min. Each membrane was then blocked and incubated with a monoclonal anti-*MYC* antibody (clone 9E10, Santa Cruz Biotechnology) at room temperature for 1 h or at 4°C for overnight. Each blot was washed and incubated in buffer containing an anti-mouse IgG antibody (1:20,000) at room temperature for 1 h. Finally, each blot was soaked in enhanced chemiluminescent reagents (GE Global Research) for 1 min and exposed to an X-ray autoradiography film for 1 min to 1 h.

Bromodeoxyuridine DNA analysis. The effects of siRNAs on cell cycle were assessed by measuring bromodeoxyuridine (BrdUrd) incorporation during a 30-min pulse 2 days after siRNA transfection. Cells were pulsed with 10 μL of 1 mmol/L stock BrdUrd added to 1 mL culture medium in each well of a 24-well plate. Cells were subsequently trypsinized, fixed in 70% ethanol, and stored in 4°C for at least 1 h. The cells were pelleted, resuspended in 0.08% pepsin (in 0.1 N HCl), and incubated at 37°C for 20 min to free nuclei. HCl (2 N) was then applied to nuclei to denature dsDNA and neutralized with 2 volumes of 0.1 mol/L sodium borate. The nuclei were then incubated on ice with 1:5 dilution of a FITC-labeled anti-BrdUrd antibody (Becton Dickinson Immunocytometry Systems) for at least 30 min and stained with 50 μg/mL of propidium iodide at 37°C for at least 15 min. BrdUrd/DNA distributions were measured in a Becton Dickinson FACSCalibur flow cytometer (fluorescence-activated cell sorting). Alternately, cells were fixed with 70% ethanol after 30 min of BrdUrd labeling for at least 2 h in room temperature, stained with mouse anti-BrdUrd antibody (BD Biosciences) and Alexa Fluor 488 goat anti-mouse (Invitrogen) antibody, and counterstained with Hoechst 33342 (Sigma-Aldrich). Cells were scanned and recorded using a Cellomics High Content

[13] http://www.affymetrix.com

[14] http://www.idtdna.com

Imaging System (KineticScan; ref. 18). Both flow and image data were analyzed to determine the fractions of G_1, BrdUrd-incorporating S-phase, and G_2-M cells as described (11, 18).

Apoptosis. The apoptotic effect of siRNA silencing was assessed using high-content image analysis. At each time point, cells were either directly stained with 1 μmol/L YO-PRO-1 stain (Invitrogen) and 10 μg/mL Hoechst 33342 for 30 min at 37°C or fixed in 4% formaldehyde at room temperature and stained with Alexa Fluor 488-phalloidin (Invitrogen) for filamentous actin (F-actin) and 10 μg/mL Hoechst 33342 for nuclei. Apoptotic cells were detected and analyzed using Cellomics Multiparameter Apoptosis and Multiparameter Cytotoxicity Bioapplications for F-actin content and YO-PRO-1 DNA staining, respectively. Intensities of YO-PRO-1 and F-actin in cells treated with siRNA were analyzed and compared with those of cells treated with LipofectAMINE only or siGFP and siControl with appropriate Cellomics applications. Significance was determined using a Student's *t* test.

Viable cell count analysis. Cell number was measured at 8, 24, and/or 48 h after treatments using the CellTiter-Glo Luminescent assay (Promega) according to the manufacturer's instructions, and luminescence was recorded with a luminometer (BioTek FLx800, BioTek Instruments, Inc.).

5′-Rapid amplification of cDNA ends for determination of* PVT1 *transcript structure. The 5′ NH_2-terminal sequences of *PVT1* transcripts were determined using 5′-rapid amplification of cDNA ends (5′-RACE) with total RNA from epithelial cells surgically scraped from normal ovary surface epithelium (OSE1157), an OSE cell line with extended life span in culture due to the transfection of SV40 large T antigen (IOSE29), and two immortalized ovarian cancer cell lines (CAOV4 and HEY). The reactions were carried out using a FirstChoice RLM-RACE kit (Ambion) following the manufacturer's instructions. Single-band PCR products from 5′-RACE were gel purified and cloned using a TOPO TA cloning kit (Invitrogen). Plasmids containing the desired 5′-RACE PCR product were isolated and purified from single bacterial colonies. They were then sequenced with M13 forward and reverse sequence primers. The sequences of individual *PVT1* exons were queried on the Web site[15] for potential "stem-loop" structures commonly observed in microRNAs (miRNA; refs. 19, 20).

Results

Genome copy number and transcriptional analyses. We applied fluorescence *in situ* hybridization (Fig. 1A) for analysis of 380 ovarian tumors arranged in tissue microarrays with probes to the MYC locus (8q24) and the chromosome 8 centromere. This analysis showed that a MYC locus copy number to centromere copy number ratio of ≥1.5 (amplification) was significantly higher in serous tumors ($P < 0.0001$) and was associated with reduced survival duration ($P = 0.0170$; Fig. 1B).

We assessed the mechanisms by which amplification at 8q24 contributes to ovarian and breast pathophysiology by analyzing the effects of reducing expression levels of transcripts encoded in the region of recurrent amplification in cell lines with and without amplification at this locus. We identified ovarian cell lines amplified at this locus by applying array comparative genomic hybridization to 30 ovarian cancer cell lines. Most regions of recurrent genome copy number abnormality, including amplification at 8q24 in the cell lines, were similar to those in primary serous ovarian tumors (Fig. 1C and D).[16] The raw array comparative genomic hybridization data have been deposited to Tab2MAGE ArrayExpress (accession no. E-TABM-246).[17] Supplementary Table S3 describes similarities in recurrent genome copy number abnormalities between the cell lines and primary tumors. Figure 1E and F shows that the genome copy number profiles at 8q24 for several ovarian tumors and cell lines are similar and suggest a consensus region of amplification spanning ~1 Mbp encoding *MYC* and *PVT1*.

We also analyzed mRNA expression of ~17,000 transcripts using Affymetrix Hu_U133A GeneChip microarrays in the 30 ovarian cancer cell lines [raw image .cel files and analyzed robust multiarray average data have been deposited to Tab2MAGE ArrayExpress (accession no. E-TABM-254)][17] and calculated Pearson's correlations between transcription levels and genome copy number changes to identify transcripts that were significantly deregulated by the genome copy number aberrations in the collection of cell lines. Each transcript was paired with a BAC clone that was nearest to the gene in the genome. These analyses revealed 417 transcripts with Pearson's correlations of >0.5 in both cell lines and in primary ovarian tumors,[16] suggesting that the cell lines mirror much of the genome copy number–driven transcriptional deregulation found in primary tumors. The genes are listed in Supplementary Table S4. We used QPCR to analyze the expression levels of 57 transcripts (listed in Supplementary Table S2) encoded in regions of recurrent copy number abnormality previously implicated in the pathophysiology of ovarian cancer. We analyzed these transcript levels in 21 cell lines (bold highlighted in Supplementary Table S1) to determine the accuracy with which the microarray analyses estimated expression levels. Supplementary Figure S1 shows correlation coefficients between QPCR and microarray results calculated for each gene in the 21 ovarian cancer cell lines. The correlation coefficients between expression levels measured using QPCR and Affymetrix array analysis were mostly high (average correlation coefficient, 0.75), except for five genes, including *PVT1*, for which the correlation coefficients were very low to negative.

Because we observed some discordances between transcript levels measured using QPCR and Affymetrix expression array analysis, we measured transcript levels of the transcripts for PVT1 and MYC using QPCR in 20 ovarian cancer cell lines. The Affymetrix U133A arrays used in this study carried probe sets 216240_at and 216249_at that were designed from EST clone M34428. The array signals for both probe sets were either undetectable or very low across all the lines, whereas the Taqman analyses designed from the same source EST sequence detected significant and variable expression levels in the same cell lines (Table 1). The Pearson's correlation between *PVT1* expression levels measured by microarray and by QPCR was only -0.02 and -0.01 for 216240_at and 216249_at, respectively, whereas the correlation between *PVT1* transcript levels measured using QPCR and genome copy number at 8q24 was high (Table 1). We attribute these discordances to the poor performance of the probe sets for *PVT1* on the microarrays. Table 1 compares array comparative genomic hybridization measurements of genome copy number at 8q24 and QPCR analyses of expression levels for *PVT1* and *MYC* in 20 of the ovarian cancer cell lines. Genome copy number was assessed at the BAC array probe closest to *PVT1* and *MYC* (clone

[15] http://microrna.sanger.ac.uk/sequences/search.shtml

[16] W-L. Kuo, et al. Genomic deregulation of transcription in serous ovarian cancers; prognostic markers and therapeutic targets, submitted for publication.

[17] http://www.ebi.ac.uk/cgi-bin/microarray/tab2mage.cgi

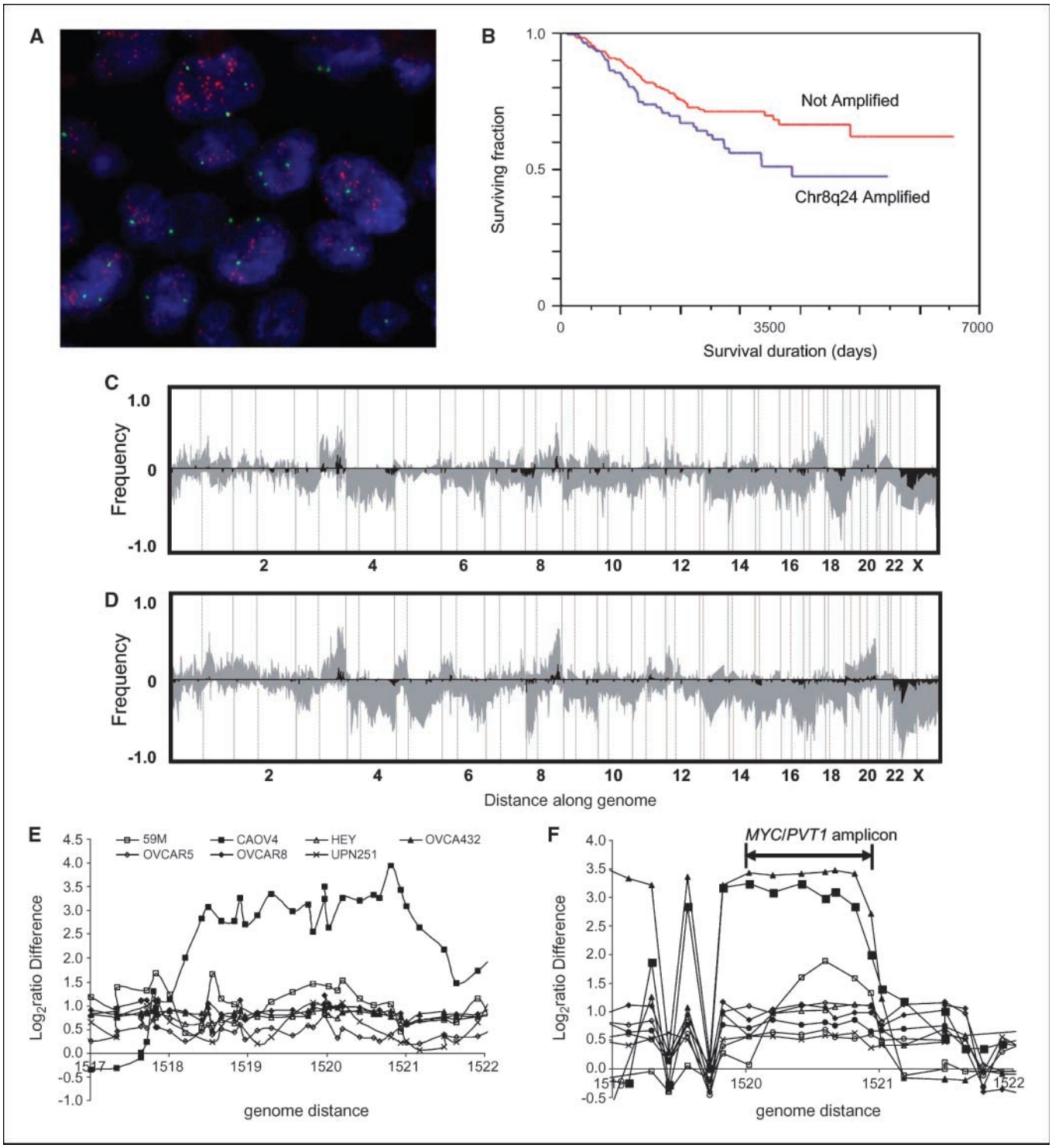

Fig. 1. Recurrent copy number aberrations in ovarian tumors and cell lines. *A,* relative amplification of the chromosome 8q24 locus determined using fluorescence *in situ* hybridization with a spectrum orange – labeled probes for MYC (*red*) and a spectrum green – labeled probe for centromere of chromosome 8 (*green*) in a mucinous tumor case (probes from Vysis). The ratio of the number of copies of the MYC probe relative to the number of copies of centromere 8 was 6.8 in this case, indicating high level of amplification. *B,* Kaplan-Meier plot showing survival rates in 380 stage I to III ovarian tumors with and without amplification of chromosome 8q24 detected by fluorescence *in situ* hybridization. *C* and *D,* frequencies of significant increases or decreases in genome copy numbers are plotted as a function of genome distances of University of California at San Francisco July 2003 freeze (National Center for Biotechnology Information Build 34) for 30 cell lines (*C*) and primary tumors from study B of Kuo et al. (Genomic deregulation of transcription in serous ovarian cancers; prognostic markers and therapeutic targets, submitted for publication). *D,* positive values indicate frequencies of samples showing copy number increases and negative values indicate frequencies of samples showing copy number decreases. Gray bars, frequencies of $\log_2$ copy numbers >0.3 or <-0.3; black bars, frequencies of $\log_2$ copy numbers >0.9 or <-0.9. Solid vertical gray lines, chromosome boundaries; dotted vertical lines, centromere locations. Bottom, numbers of the even-numbered chromosomes. Data are arranged with chromosome 1pter to the left and chromosomes Xqter to the right. *E,* $\log_2$ copy number changes in seven ovarian cell lines that had amplification on chromosome 8q24. *F,* $\log_2$ copy numbers in ovarian tumors (Kuo et al. Genomic deregulation of transcription in serous ovarian cancers; prognostic markers and therapeutic targets, submitted for publication) showing copy number increases at 8q24. The *MYC*/*PVT1* amplicon was defined by the minimal overlapping regions from tumors.

Table 1. Expression levels of *PVT1* and *MYC* and genome copy number changes at 8q24 in ovarian cancer cell lines

Cell line name	PVT1	Clone VYS08A2679	c-myc
	Taqman expression (normalized to the expression of Stratagene RNA reference pool)	Copy number changes	Taqman expression (normalized to the expression of Stratagene RNA reference pool)
A2780	0.91	-0.17	1.14
CAOV3	0.91	-0.04	0.09
CAOV4*	21.36	3.15	2.49
DOV13	2.05	-0.07	0.60
ES-2	1.29	0.32	0.86
HEY*	5.09	0.63	2.88
OCC1	0.67	-0.44	0.30
OV90	0.25	-0.02	0.62
OVCA420	1.89	0.54	1.92
OVCA429	3.28	0.09	0.72
OVCA432*	7.18	0.91	1.25
OVCA433	3.14	0.04	0.62
OVCAR3	1.47	0.52	0.45
OVCAR5	2.93	0.73	1.24
OVCAR8*	3.54	1.09	1.00
PA-1	2.55	-0.01	0.80
SKOV3	0.70	0.09	0.76
SW626	1.95	0.22	1.63
TOV112D	1.25	0.40	1.19
TOV21G	5.74	0.00	0.82
Correlation coefficient	$r^2 = 0.89$		$r^2 = 0.64$

*Cell lines with both overexpression and amplification of PVT1.

VYS08A2679). The starting site of this BAC clone overlaps with 5′ end of the *MYC* locus and 3′ end of the clone is ~50 kb downstream of the 5′ end of the *PVT1* transcription unit. Both *PVT1* and *MYC* transcript levels were strongly correlated with genome copy number in the 20 ovarian cancer cell lines tested. Interestingly, the correlation between copy number and expression level was higher for *PVT1* than for *MYC* (0.89 and 0.64, respectively). This is due to the fact that some cell lines (e.g., OVCA432 and OVCAR8) with amplification at 8q24 did not overexpress *MYC*, whereas transcription levels of *PVT1* were high in all lines (e.g., CAOV4, HEY, OVCA432, and OVCAR8), showing amplification at 8q24. In most cell lines, transcription levels of *MYC* and *PVT1* were significantly higher where they were amplified than in cell lines in which they were not. However, *PVT1* was highly expressed in cell line TOV21G, although it was not amplified, suggesting another mechanism of overexpression. We also compared transcription levels of *PVT1* in 18 different normal tissues, 3 breast cancer lines (SKBR3, HBL100, and SUM159T), and 2 normal ovarian cell lines (OSE1157 and IOSE29) with those in two 8q24-amplified ovarian cancer lines (CAOV4 and HEY) using QPCR. *PVT1* was expressed in several of the tissues tested with highest expression in trachea but not at levels found in the two ovarian cancer cell lines. Breast cell lines generally expressed *PVT1* at much lower levels than ovarian cells.

We did 5′-RACE with cDNA from OSE1157, IOSE29, CAOV4, and HEY cells. Analyses of the intensities of bands generated by 5′-RACE PCR products along with QPCR analyses showed that expression of *PVT1* in OSE1157 cells was significantly lower than that in IOSE29 cells and >20-fold lower than that in HEY and CAOV4 cells. Single bands of ~350 bp were only observed in 5′-RACE PCR products from OSE1157 and HEY cells. The 5′-RACE of IOSE29 and CAOV4 cells produced multiple bands. The single bands from OSE1157 and HEY cells were cut, gel purified, cloned into TOPO TA cloning vectors, and sequenced with M13 primers flanking the inserted PCR products. Two different sequences (#1 and #2 in Supplementary Fig. S2) were obtained from OSE1157 5′-RACE. Only one sequence was detected in plasmids isolated from six bacterial colonies that were transformed with 5′-RACE PCR products from HEY cells. The HEY sequence was identical to the 5′-RACE sequence #2 from OSE1157. We then searched human EST databases using National Center for Biotechnology Information nucleotide-nucleotide BLAST (blastn) based on our 5′-RACE sequences and the sequence of a cDNA clone (National Center for Biotechnology Information accession no. BC033263) that was previously considered to be a full-length clone for *PVT1*. The 125 bp at the 3′ ends of both 5′-RACE sequences overlapped with the 5′ end of the BC033263 sequence. ESTs that had >95% sequence homology with the query sequences were assembled to predict full-length transcripts. The web tool, NIX (Nucleotide Identify X software),[18] was used to identify exons from these EST alignments. Nine exons were predicted for each of the two *PVT1* full-length transcripts (Fig. 2) assembled from sequences of 5′-RACE #1 and #2 and BC033263. The two transcripts shared exons 2 to 9 but had different first exons. We termed the first exon that corresponds to 5′-RACE sequence #1 as exon 1a and the exon that corresponds to 5′-RACE sequence #2 as exon 1b. Exon 1a is upstream of exon 1b in the genome (Fig. 2). To determine whether the predicted full-length transcripts exist in the

[18] http://www.hgmp.mrc.ac.uk/NIX

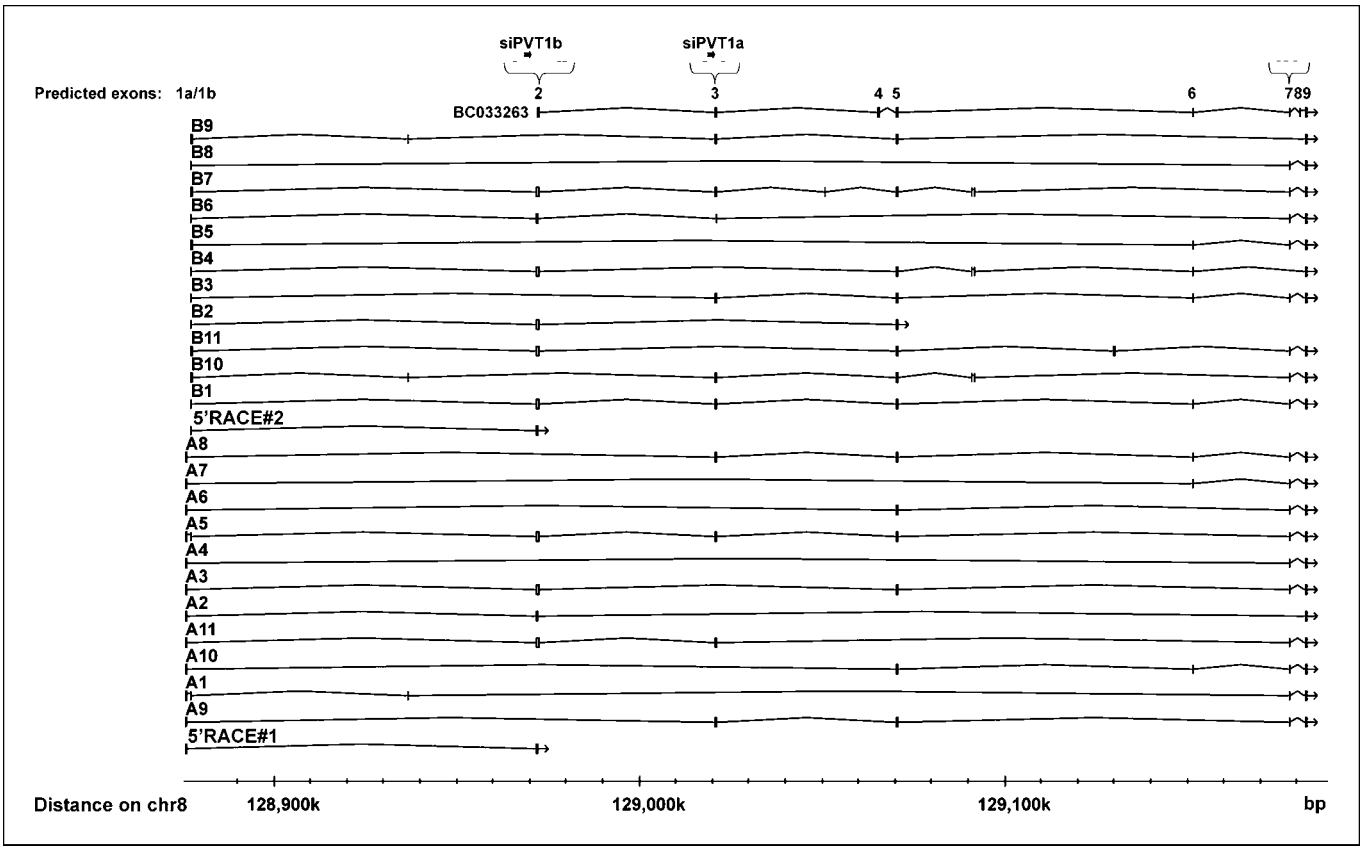

Fig. 2. Genomic mapping of *PVT1* transcripts identified from HEY cells and normal testis and alignment of siRNAs against *PVT1*. Bottom, chromosome distance coordinates in kb from National Center for Biotechnology Information Build 36.2 of the *PVT1* locus. Box, segment of cDNA sequence from a transcript; lines in between, genomic sequence. The arrow at the end of each transcript points to the direction of transcription, which in all cases are in the sense direction. Transcripts A1 to A11 are PCR products amplified with primers against predicted exon 1a and exon 9. Transcripts B1 to B11 are PCR products amplified with primers against predicted exon 1b and exon 9. The positions of the 5′-RACE sequences #1 and #2 and the EST clone BC033263 are also mapped for reference. Top, position of nine predicted exons from full-length transcript A and transcript B. The predicted exons 2, 3, and 7 are magnified to show alignments of *PVT1* siRNAs. Block arrowheads, siPVT1a and siPVT1b used in this study that have shown significant knockdown of *PVT1* mRNA levels in multiple cell lines. Light gray horizontal lines, other siRNAs that did not show significant knockdown of *PVT1* transcription.

transcriptome, primers against exon 1a or 1b and exon 9 were used to amplify *PVT1* cDNAs from the HEY cells and normal testis. PCR products were then cloned and sequenced. As shown in Fig. 2, multiple alternatively spliced variants were identified from these PCR products. Predicted exons 4 and 8 were missing in all of the 22 PCR products that we have cloned. We also assessed the sequences of individual *PVT1* exons detected by PCR for possible stem-loop structures that could signify the presence of transcripts that will be bound and cleaved by Drosha to liberate ~70-nucleotide miRNA precursors (21). Sequences homologous to known stem-loop structures in different species were found in predicted exons 5, 6, 7, and 9; however, the significance indices of these predictions were low in all cases.

Biological responses to inhibition of PVT1 and MYC expression. Because our main goal in this study was to determine how *PVT1* and MYC contribute to ovarian cancer pathophysiology when overexpressed by amplification or other genomic mechanisms, we compared biological responses to inhibition of *PVT1* and *MYC* in ovarian and breast cancer cell lines with and without amplification and overexpression of these two genes.

We assessed the biological effects of inhibiting mRNA levels of *PVT1* using siRNAs in the ovarian cancer cell lines CAOV4, HEY, OVCA432, and OVCAR8 where 8q24 is amplified and *PVT1* is overexpressed and in cell lines A2780, CAOV3, OV90, and SKOV3 where *PVT1* is not amplified or overexpressed. We compared these responses to responses to siRNA inhibition of *MYC* expression in a subset of these lines. After 48 h, >50% knockdown in *PVT1* mRNA level was achieved in all ovarian cancer lines treated with 120 nmol/L siPVT1a and at least 80% knockdown was achieved in HEY cells treated with either 120 nmol/L siPVT1a or siPVT1b. Representative semiquantitative reverse transcription-PCR agarose gel electrophoresis and Taqman QPCR analyses of *PVT1* are shown in Fig. 3A and B, respectively. Figure 3A also shows similar *PVT1* knockdown levels in three breast cancer cell lines (SUM159PT, HBL100, and SKBR3). Notably, siRNA knockdown of *PVT1* expression was accompanied by a slight decrease in *MYC* protein expression in CAOV4 but not in any of the other cell lines (Fig. 3C). Figure 3C shows that 200 nmol/L siMYCa also reduced the level of *MYC* protein expression to >50% at 48 h. To minimize off-target effects of high concentration of siRNA, we also assessed responses to a different siRNA against *MYC* (siMYCb) that reduced the *MYC* mRNA level in HEY cells to <12% of that in siControl-transfected cells (Fig. 3D) at 120 nmol/L. Eight other siRNAs targeting different parts of *PVT1* transcript (see Fig. 2) were also tested for knockdown in HEY cells but none of these reduced *PVT1* mRNA levels significantly.

Knockdown of PVT1 or MYC inhibits proliferation. We determined the effects of *PVT1* and/or *MYC* knockdown on

cell proliferation by measuring changes in fractions of cells in the G_1, S, and G_2-M phases of the cell cycle estimated from BrdUrd/DNA distributions measured for cells pulse labeled with BrdUrd at 8, 24, and/or 48 h after siRNA transfection and by counting viable cells using the CellTiter-Glo Luminescent assay that measures ATP levels in metabolically active cells. Table 2 shows that siPVT1a strongly inhibited BrdUrd incorporation in four *PVT1*-amplified/overexpressed cell lines but not in any of the nonamplified lines at 48 h. In HEY and OVCAR8, the reduction in the fraction of cells in S phase was accompanied by a significant accumulation of cells in G_1 phase of the cell cycle. Treatment with 120 nmol/L siPVT1a and 200 nmol/L siMYCa produced similar levels of inhibition of BrdUrd incorporation in CAOV4 and HEY cells in which both *PVT1* and *MYC* are amplified and overexpressed (Table 2). Neither G_1 cell cycle arrest nor reduction in S phase was seen in any of the four *PVT1*/*MYC*-nonamplified/overexpressed cell lines. siPVT1b had even stronger antiproliferation effects in CAOV4 and HEY cells than siPVT1a (Table 2). We also evaluated the effect of siRNA knockdown with siPVT1a on cell growth using CellTiter-Glo Luminescent assays. Table 2 shows that the number of viable cells in siPVT1a-transfected HEY cells started to decrease relative to that of cells treated with LipofectAMINE alone or siControl at 8 h. By 24 h, the viable cell count was only 40% of that of control cultures. In contrast, siPVT1a had no effect on cell viability in two ovarian cell lines in which *PVT1* was not amplified or overexpressed.

To determine the generality of the phenotype resulting from *PVT1* knockdown, we also compared the effect of siPVT1a transfection in two breast cancer cell lines (SUM159PT and HBL100) in which *PVT1* is both amplified and overexpressed with that in a breast line (SKBR3) where *PVT1* is only amplified but not overexpressed. As shown in Table 2, transfection of siPVT1a decreased the proportion of BrdUrd-incorporating cells in SUM159PT and HBL100 but not in SKBR3.

Knockdown of PVT1 but not MYC increases apoptosis. We assessed the effects of inhibiting *PVT1* expression on programmed cell death in cells with and without *PVT1* amplification/overexpression by measuring membrane permeability (22), cell morphology, and F-actin reorganization (23, 24) using high-content image analyses. YO-PRO-1 dye uptake increases when cells lose membrane integrity during cell death, whereas F-actin reorganization results in increased Alexa Fluor 488-phalloidin binding that has been associated with earlier stages of apoptosis (24). Beginning at 8 h after transfection, siPVT1a significantly increased YO-PRO-1 dye uptake and F-actin staining relative to LipofectAMINE controls in HEY and CAOV4 cell lines in which *PVT1* is amplified and overexpressed (Fig. 4A and B). Increased apoptosis in siPVT1a-transfected cells was further confirmed with Annexin V staining in CAOV4 cells (data not shown). In contrast, transfection of siPVT1a in three of the four nonamplified/overexpressed lines produced no significant changes, except in SKOV3 cells where F-actin staining increased significantly after

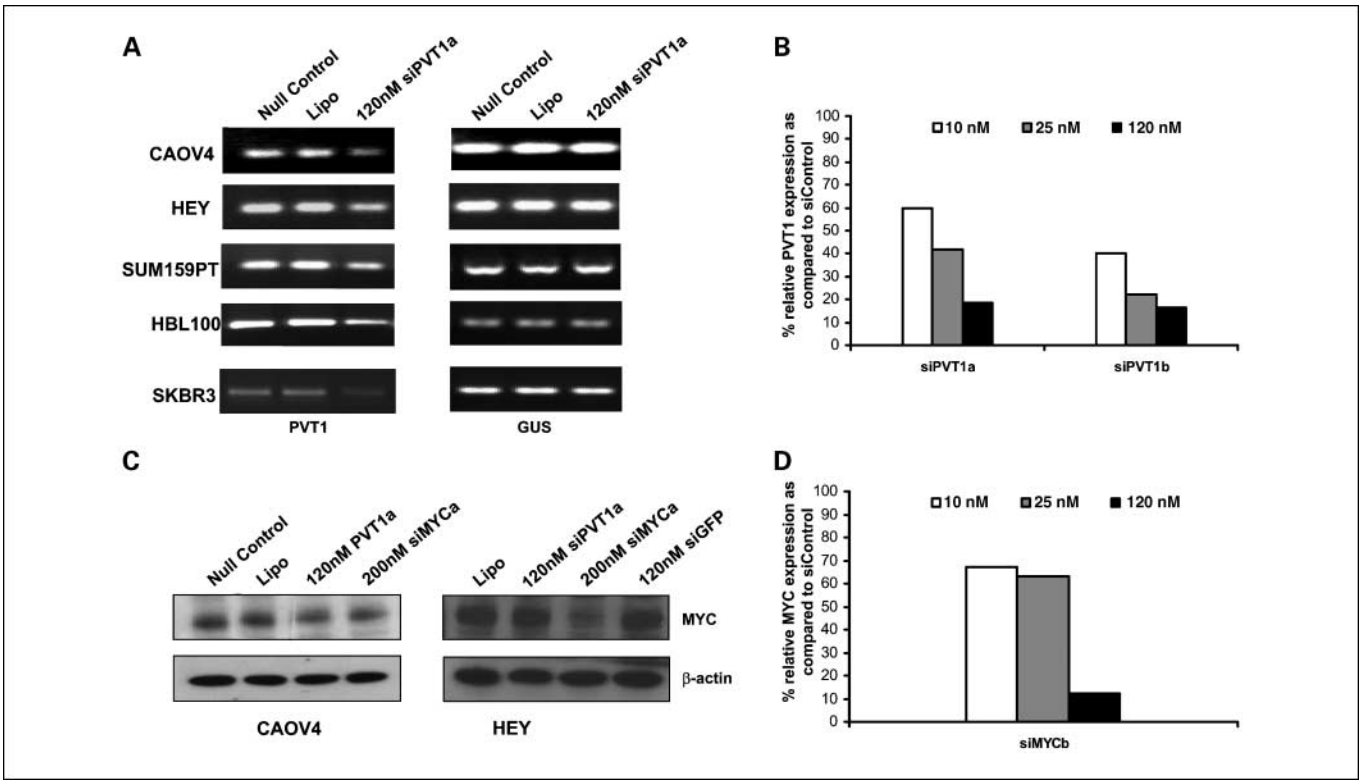

Fig. 3. Expression of *PVT1* and *MYC* in control and siRNA-treated cells. *A,* agarose gel electrophoresis images of semiquantitative reverse transcription-PCR specific for *PVT1* transcript in CAOV4, HEY, SUM159PT, HBL100, and SKBR3 cells treated with conditions as indicated. GUS expression was tested as the sample loading control. *B,* % *PVT1* mRNA level knockdown measured by Taqman QPCR in HEY cells transfected with three concentrations (as indicated in the graph) of siPVT1a and siPVT1b compared with cells transfected with siControl. *C,* Western blots with anti-*MYC* antibody in CAOV4 and HEY cells transfected with siPVT1a and siMYCa. In these experiments, the null control was cells that were incubated with Opti-MEM only during transfection. The LipofectAMINE (*Lipo*) control was cells that were mock transfected with LipofectAMINE 2000 at a maximum concentration used in each experiment (5-7.5 mg/mL). *D,* % *MYC* mRNA level knockdown measured by Taqman QPCR in HEY cells transfected with different concentrations (as indicated in the graph) of siMYCb compared with cells treated with siControl.

Table 2. Effects of *PVT1* and *MYC* siRNAs on cell proliferation in ovarian and/or breast cancer cell lines

BrdUrd cell cycle FACS analysis

Average % distribution (n = 2 or 3)

MYC/PVT1 amplified		Lipo	120 nmol/L siGFP	120 nmol/L siPVT1a	200 nmol/L siMYCb
CAOV4	G_1	56	48	60	56
	S	17	19	2	7
HEY	G_1	44		66	61
	S	41		1	4
OVCA432	G_1	36	43	53	
	S	39	33	9	
OVCAR8	G_1	25	26	57	
	S	42	45	3	

MYC/PVT1 nonamplified		Lipo	120 nmol/L siGFP	120 nmol/L siPVT1a	200 nmol/L siMYCb
A2780	G_1	33	31	35	
	S	49	49	48	
CAOV3	G_1	58	60	58	
	S	24	21	22	
OV90	G_1	51		47	43
	S	32		30	35
SKOV3	G_1		39	42	
	S		17	17	

CTG assay

Average % viable cell count vs Lipo control (n = 4)

MYC/PVT1 amplified		120 nmol/L siControl	120 nmol/L siPVT1a
HEY	8 h	104	64
	24 h	86	40
	48 h	104	45

MYC/PVT1 nonamplified		120 nmol/L siControl	120 nmol/L siPVT1a
A2780	8 h	100	107
	24 h	97	144
	48 h	92	98
OV90	8 h	100	111
	24 h	107	105
	48 h	106	104

Cellomics BrdUrd incorporation assay

Average % BrdUrd proportion, S phase (n = 4)

PVT1 overexpressed	120 nmol/L siControl	120 nmol/L siPVT1a	120 nmol/L siPVT1b	120 nmol/L siMYCb
CAOV4	34	12	0.4	9
HEY	30	4	3	
SUM159PT	52	16		
HBL100	21	11		

PVT1 nonoverexpressed	120 nmol/L siControl	120 nmol/L siPVT1a	120 nmol/L siPVT1b	120 nmol/L siMYCb
OV90	12	30	23	14
SKBR3	16	19		

NOTE: BrdUrd/propidium iodide cell cycle distributions were measured by fluorescence-activated cell sorting analyses or by Cellomics High Content Imaging System. Viable cell counts were assessed using the CellTiter-Glo Luminescent cell viability assay.
Abbreviations: FACS, fluorescence-activated cell sorting analysis; CTG, CellTiter-Glo Luminescent; Lipo, LipofectAMINE.

siPVT1a transfection (P = 0.001). Apoptosis induced by siRNA knockdown of *PVT1* expression was more pronounced in CAOV4 and HEY cells transfected with siPVT1b compared with cells transfected with siPVT1a. No effect on apoptosis was seen in the nonamplified cell line OV90 transfected with either siPVT1a or siPVT1b (Fig. 4C). Transfection with 120 nmol/L siMYCb did not significantly affect apoptosis in any of the cell lines tested (Fig. 4B and C). Increased apoptosis was also seen in the breast cancer cell lines in which *PVT1* was amplified and overexpressed following transfection of siPVT1a but not in SKBR3 where *PVT1* was not overexpressed (data not shown). We also treated the eight ovarian cell lines with paclitaxel as a positive control for apoptosis induction. Paclitaxel (100 nmol/L) induced massive apoptosis in six of the eight cell lines as expected, with the exception of two PVT1-amplified/overexpressed cell lines (HEY and OVCA432; Fig. 4A).

Discussion

Several published findings implicate *PVT1* in aspects of cancer pathophysiology. Examples include observations that rearrangement of the region at 8q24 encoding *MYC* and *PVT1* is frequently involved in human leukemias and lymphomas (4, 5), the regions is frequently amplified in solid tumors (2), and a site of recurrent tumorigenic viral integration in mice (25). *MYC* is well established as an oncogene in this region. We now provide functional evidence for the importance of increased expression of *PVT1* in cancer through analysis of cell lines with and without amplification at 8q24. These cell lines were selected from a collection of 30 ovarian cell lines described in this article and 51 breast cancer cell lines described elsewhere (11). Our analyses of both collections show that the recurrent genome aberrations and the resulting deregulation of gene expression are highly concordant between primary tumors and the cell lines. Thus, the aspects of amplification-dependent cancer pathophysiology discovered in the cell lines are likely to be obtained in primary tumors as well.

The strongest evidence for the importance of *PVT1* in cancer pathophysiology is our observation that siRNA silencing of *PVT1* expression decreases cell proliferation and increases apoptosis in breast and ovarian cancer cell lines in which it was amplified and overexpressed but not in cell lines where it is not amplified/overexpressed. The amplification/overexpression-specific response phenotypes argue that the observed effects are due to down-regulation of *PVT1* rather than to off-target effects of siRNA. The *PVT1* specificity of the response is further

supported by our observation that the same amplification/overexpression-specific response phenotype was seen using two different siRNAs against *PVT1*.

PVT1 has been suggested to function as a *MYC* activator. However, our demonstration that *PVT1* inhibition does not alter *MYC* levels in most of the cell lines where it influences both apoptosis and proliferation argues against this. Moreover, inhibition of *PVT1* but not *MYC* induces apoptosis in cell lines where they are both amplified and overexpressed. If *PVT1* were acting through *MYC*, the apoptotic response should have been observed after inhibition of *MYC*. Therefore, we conclude that *PVT1* acts independently of *MYC* in generation of the apoptotic phenotype.

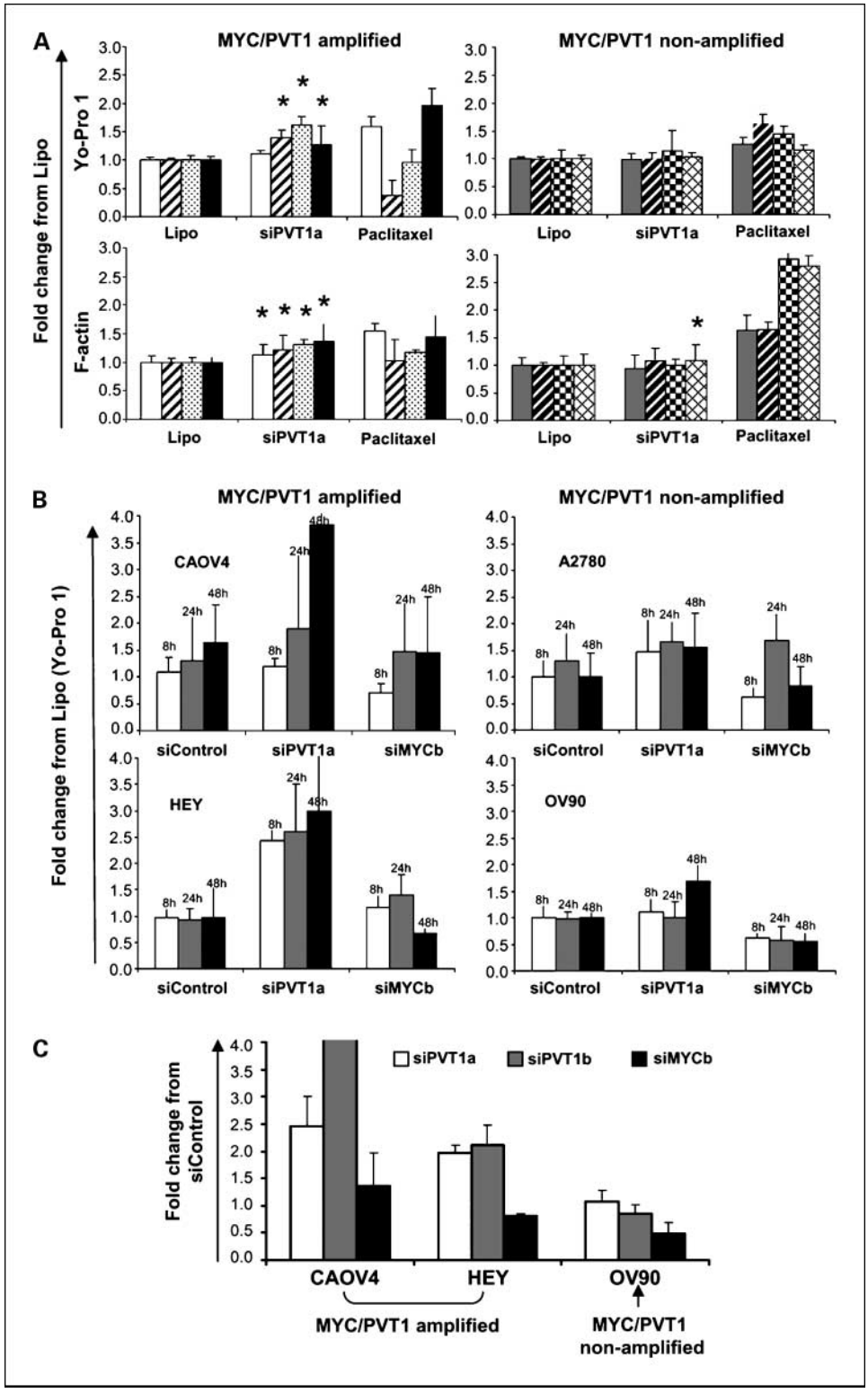

Fig. 4. Effects of *PVT1* and *MYC* siRNAs on apoptosis in ovarian and/or breast cancer cell lines measured by the Cellomics High Content Imaging System. *A,* cell permeability (YO-PRO-1 dye intake) and microfilament reorganization (F-actin staining) in *PVT1*-amplified/overexpressed and *PVT1*-nonamplified ovarian cell lines treated with siPVT1a and paclitaxel for 48 h. For the amplified lines, the white columns represent data from CAOV4, the columns with black stripes are for HEY, the dotted columns are for OVCA432, and the solid black columns represent results from OVCAR8. For nonamplified cell lines, the gray columns represent data from A2780, the columns that have white hatched stripes against a black background represent CAOV3, the columns with checkered pattern are for OV90, and the columns with cross-hatched lines represent data from SKOV3. *B,* apoptosis induced by transfection of 120 nmol/L siPVT1a at 8, 24, and 48 h in *PVT1*-amplified/overexpressed and *PVT1*-nonamplified ovarian cell lines. All the siRNAs were transfected at 120 nmol/L concentration. The heights of the columns in bar graphs represent fold changes in apoptotic cell proportions from LipofectAMINE-treated cells. *, experiments in which the difference in total fluorescent intensity was significant between siPVT1a-transfected cells and Lipofect-AMINE-treated control cells ($P < 0.05$). *C,* comparison of apoptotic effects (measured by YO-PRO-1 dye intake) induced by 120 nmol/L siPVT1a and siPVT1b transfection at 48 h in three ovarian cell lines.

The strong induction of apoptosis resulting from siRNA inhibition of *PVT1* suggests that *PVT1* amplification contributes to the oncogenic phenotype, at least in part, by suppressing apoptosis. This suggests the interesting possibility that amplification at 8q24 might have two simultaneous oncogenic functions: overexpression of *MYC*, which stimulates proliferation, and overexpression of *PVT1*, which not only stimulates proliferation but also inhibits the apoptotic response normally associated with overexpression of *MYC*. The apoptosis suppression function of *PVT1* may also explain why its overexpression is associated with reduced survival duration in patients treated with platinum plus taxane–based therapies. Platinum compounds produce apoptotic responses through production of DNA cross-links (26), whereas taxanes trigger apoptotic responses by stabilizing otherwise dynamic microtubules that are important for centrosome and mitotic spindle function (27). Overexpression of *PVT1* may contribute to resistance to these agents by suppressing the apoptotic mechanisms through which they work. This possibility is partially supported by our finding that two ovarian cancer cell lines with high-level *PVT1* expression do not exhibit significant apoptotic responses to treatment with paclitaxel at concentrations that induced apoptosis in the other cell lines. However, *PVT1* is not the only determinant of response because two other *PVT1*-amplified/overexpressed cell lines exhibit a significant apoptotic response to paclitaxel.

Elucidation of the mechanism(s) by which *PVT1* overexpression contributes to suppression of apoptosis and proliferation is complicated by the fact that *PVT1* is transcribed into multiple splice forms that vary in form and abundance between cell lines (data not shown; ref. 9). However, our observation that siRNAs complementary to sequences in exons 2 and 3 both produced phenotypes that were specific to cell lines with amplification and overexpression of *PVT1* suggested that transcripts containing these two exons are functionally important.

Mechanistic interpretation is further complicated by the observation that *PVT1* seems to be a noncoding RNA because the longest open reading frame predicted from our assessment of *PVT1* sequences is 150 amino acids encoded in the first two exons. The noncoding RNAs most strongly implicated in cancer thus far are miRNAs (28). These 20- to 22-nucleotide RNAs are the result of enzymatic processing of larger transcripts and may operate in cancer by blocking translation of target genes to which they are complementary. Deregulated expression of several miRNAs has been associated with poor disease outcome in chronic lymphocytic leukemia, colorectal neoplasia, lung cancer, and Burkitt's lymphoma (28). miRNAs are also frequently located at fragile sites and genomic regions that involved cancers (29). Thus, we investigated the possibility of *PVT1* as a miRNA. Our computational analyses show that the predicted sequences of *PVT1* transcripts do not seem to have the stem-loop structures normally associated with miRNAs (20, 30, 31). A recent study by Dr. Huppi has identified seven putative miRNAs within the ~400-kb *PVT1* genomic locus.[12] The precursor sequence of one of these overlaps with exon 1b in our current study, but it also extends beyond the consensus splice site of the exon. The precursor sequences of the other six miRNAs have no association with any of the annotated *PVT1* exons and might be results of extensive alternative splicing found in this locus (Fig. 2).[12] This may explain our failure to identify potential miRNA precursor sequences in our predicted *PVT1* transcripts, which contain mostly known exons. Thus, the mechanism by which *PVT1* exerts its pathologic function remains unclear.

In conclusion, we have used our well-characterized cell line collection to show that amplification at 8q24 increases expression of both *MYC* and *PVT1* and that both of these deregulated transcripts seem to contribute to ovarian and breast cancer pathophysiology. We have shown that *PVT1* is most likely a noncoding RNA that acts independently of *MYC* and, when amplified and overexpressed, acts to increase proliferation and inhibit apoptosis.

Acknowledgments

We thank Drs. Richard E. Neve, Michael McManus, Eric A. Collisson, Konrad Huppi, and Natasha J. Kaplen for helpful discussions. We thank Dr. Huppi for a prepublication copy of his manuscript on PVT1 miRNAs.

References

1. Lancaster JM, Dressman HK, Whitaker RS, et al. Gene expression patterns that characterize advanced stage serous ovarian cancers. J Soc Gynecol Investig 2004; 11:51–9.
2. Popescu NC, Zimonjic DB. Chromosome-mediated alterations of the MYC gene in human cancer. J Cell Mol Med 2002;6:151–9.
3. Shtivelman E, Henglein B, Groitl P, Lipp M, Bishop JM. Identification of a human transcription unit affected by the variant chromosomal translocations 2;8 and 8;22 of Burkitt lymphoma. Proc Natl Acad Sci U S A 1989;86:3257–60.
4. Cory S, Graham M, Webb E, Corcoran L, Adams JM. Variant (6;15) translocations in murine plasmacytomas involve a chromosome 15 locus at least 72 kb from the c-myc oncogene. EMBO J 1985;4:675–81.
5. Webb E, Adams JM, Cory S. Variant (6;15) translocation in a murine plasmacytoma occurs near an immunoglobulin κ gene but far from the myc oncogene. Nature 1984;312:777–9.
6. Graham M, Adams JM, Cory S. Murine T lymphomas with retroviral inserts in the chromosomal 15 locus for plasmacytoma variant translocations. Nature 1985; 314:740–3.
7. Graham M, Adams JM. Chromosome 8 breakpoint far 3′ of the c-myc oncogene in a Burkitt's lymphoma 2;8 variant translocation is equivalent to the murine pvt-1 locus. EMBO J 1986;5:2845–51.
8. Mengle-Gaw L, Rabbitts TH. A human chromosome 8 region with abnormalities in B cell, HTLV-I$^+$ T cell and c-myc amplified tumours. EMBO J 1987;6: 1959–65.
9. Shtivelman E, Bishop JM. The PVT gene frequently amplifies with MYC in tumor cells. Mol Cell Biol 1989; 9:1148–54.
10. Shtivelman E, Bishop JM. Effects of translocations on transcription from PVT. Mol Cell Biol 1990;10: 1835–9.
11. Neve RM, Chin K, Fridlyand J, et al. A collection of breast cancer cell lines for the study of functionally distinct cancer subtypes. Cancer Cell 2006;10:515–27.
12. Hodgson G, Hager JH, Volik S, et al. Genome scanning with array CGH delineates regional alterations in mouse islet carcinomas. Nat Genet 2001;29:459–64.
13. Hackett CS, Hodgson JG, Law ME, et al. Genome-wide array CGH analysis of murine neuroblastoma reveals distinct genomic aberrations which parallel those in human tumors. Cancer Res 2003;63:5266–73.
14. Snijders AM, Nowak N, Segraves R, et al. Assembly of microarrays for genome-wide measurement of DNA copy number. Nat Genet 2001;29:263–4.
15. Lapuk A, Volik S, Vincent R, et al. Computational BAC clone contig assembly for comprehensive genome analysis. Genes Chromosomes Cancer 2004; 40:66–71.
16. Irizarry RA, Bolstad BM, Collin F, Cope LM, Hobbs B, Speed TP. Summaries of Affymetrix GeneChip probe level data. Nucleic Acids Res 2003; 31:e15.
17. Ginzinger DG. Gene quantification using real-time quantitative PCR: an emerging technology hits the mainstream. Exp Hematol 2002;30:503–12.
18. Stilwell JL, Guan Y, Neve RM, Gray JW. Systems biology in cancer research: genomics to cellomics. Methods Mol Biol 2007;356:353–65.
19. Griffiths-Jones S. The microRNA Registry. Nucleic Acids Res 2004;32:D109–11.
20. Griffiths-Jones S, Grocock RJ, van Dongen S, Bateman A, Enright AJ. miRBase: microRNA sequences, targets and gene nomenclature. Nucleic Acids Res 2006;34:D140–4.
21. Murchison EP, Hannon GJ. miRNAs on the move:

miRNA biogenesis and the RNAi machinery. Curr Opin Cell Biol 2004;16:223–9.
22. Mingeot-Leclercq MP, Brasseur R, Schanck A. Molecular parameters involved in aminoglycoside nephrotoxicity. J Toxicol Environ Health 1995;44:263–300.
23. Levee MG, Dabrowska MI, Lelli JL Jr, Hinshaw DB. Actin polymerization and depolymerization during apoptosis in HL-60 cells. Am J Physiol 1996;271:C1981–92.
24. Okada T, Otani H, Wu Y, et al. Role of F-actin organization in p38 MAP kinase-mediated apoptosis and necrosis in neonatal rat cardiomyocytes subjected to simulated ischemia and reoxygenation. Am J Physiol Heart Circ Physiol 2005;289:H2310–8.
25. Akagi K, Suzuki T, Stephens RM, Jenkins NA, Copeland NG. RTCGD: retroviral tagged cancer gene database. Nucleic Acids Res 2004;32:D523–7.
26. Cepeda V, Fuertes MA, Castilla J, Alonso C, Quevedo C, Perez JM. Biochemical mechanisms of cisplatin cytotoxicity. Anticancer Agents Med Chem 2007;7:3–18.
27. Bergstralh DT, Ting JP. Microtubule stabilizing agents: their molecular signaling consequences and the potential for enhancement by drug combination. Cancer Treat Rev 2006;32:166–79.
28. Gregory RI, Shiekhattar R. MicroRNA biogenesis and cancer. Cancer Res 2005;65:3509–12.
29. Calin GA, Sevignani C, Dumitru CD, et al. Human microRNA genes are frequently located at fragile sites and genomic regions involved in cancers. Proc Natl Acad Sci U S A 2004;101:2999–3004.
30. McManus MT. MicroRNAs and cancer. Semin Cancer Biol 2003;13:253–8.
31. Mattick JS, Makunin IV. Non-coding RNA. Hum Mol Genet 2006;15 Spec No 1:R17–29.